Available online at www.sciencedirect.com

ScienceDirect

Energy Procedia 35 (2013) 253 – 264

Energy Procedia

DeepWind'2013, 24-25 January, Trondheim, Norway

The effect of second-order hydrodynamics on floating offshore wind turbines

Line Roald[a], Jason Jonkman[b], Amy Robertson[b], Ndaona Chokani[a]

[a]*Laboratory of Energy Conversion, ETH Zürich, Sonneggstrasse 3, 8092 Zürich, Switzerland*
[b]*National Renewable Energy Laboratory (NREL), 15013 Denver West Parkway, Golden, CO 80401, United States of America*

Abstract

Offshore winds are generally stronger and more consistent than winds on land, making the offshore environment attractive for wind energy development. A large part of the offshore wind resource is however located in deep water, where floating turbines are the only economical way of harvesting the energy. The design of offshore floating wind turbines relies on the use of modeling tools that can simulate the entire coupled system behaviour. At present, most of these tools include only first-order hydrodynamic theory. However, observations of supposed second-order hydrodynamic responses in wave-tank tests performed by the DeepCwind consortium suggest that second-order effects might be critical. In this paper, the methodology used by the oil and gas industry has been modified to apply to the analysis of floating wind turbines, and is used to assess the effect of second-order hydrodynamics on floating offshore wind turbines. The method relies on combined use of the frequency-domain tool WAMIT and the time-domain tool FAST. The proposed assessment method has been applied to two different floating wind concepts, a spar and a tension-leg-platform (TLP), both supporting the NREL 5-MW baseline wind turbine. Results showing the hydrodynamic forces and motion response for these systems are presented and analysed, and compared to aerodynamic effects.

Keywords: offshore floating wind turbine, second-order hydrodynamics, wave loads, spar buoy, tension-leg platform

1. Introduction

Designing, building and maintaining wind parks offshore requires knowledge about both the wind turbines and the marine environment in which they are to function. Important tools in the process of

* Corresponding author. Tel.: +41 44 632 65 77; fax: +41 44 632 12 52.
E-mail address: roald@eeh.ee.ethz.ch.
Current Address: Power Systems Laboratory, ETH Zürich, Physikstrasse 3, 8092 Zürich, Switzerland

doi:10.1016/j.egypro.2013.07.178

finding an optimal design for a floating turbine are computer-aided engineering (CAE) tools that simulate the turbine nonlinearly in the time domain, including aerodynamics, hydrodynamics, structural elasticity and the turbine control system. The tools that have been verified through the International Energy Agency (IEA) Wind Task 23 Offshore Code Comparison Collaborative (OC3) [9] include (among others) FAST by NREL, GH Bladed by GL Garrad Hassan and HAWC2/SIMO and Riflex by DTU Wind Energy/MarinTek.

There are several approaches to the computation of hydrodynamic loading, and among the most suitable formulations for wind turbines are the Morison's equation, an empirical formulation for inertia forces and viscous drag important to slender structures, and the radiation/diffraction approach describing effects important for large-volume structures. The latter formulation is considered here. The radiation and diffraction approach incorporates wave reflection and scattering, but ignores all viscous effects by assuming potential flow. Assuming small platform motions (relative to the waves) and a small wave slope, the radiation problem and the diffraction problem are expanded using a perturbation series with regards to the wave slope, and are split into first-order, second-order and higher-order parts. These parts can then be solved separately.

Often, only the first-order problem is solved (at least in a preliminary design) and all higher-order terms neglected, assuming that the higher-order forces will be at least an order of magnitude smaller. This significantly reduces the complexity of the problem, and the solution becomes much less computationally demanding, while it still remains reasonably accurate in most cases. Due to the linearity of the first-order problem, the first-order forces and motions oscillate at the same frequency as the incident waves.

The second-order parts of the perturbation series form the second-order hydrodynamic problem, which is the topic of interest in this paper. The second-order problem addresses interactions between two harmonically oscillating components, resulting in forces and motions at the sum and difference frequencies of the incident waves. Offshore structures are normally designed to have their eigenfrequencies outside the excitation range of the incident waves, i.e. above or below 0.25-1.25 rad/s (periods of 5-25 s). The sum- and difference-frequency forces introduce excitation above and below the frequencies of the first-order forces, and may potentially excite the eigenfrequencies of the structures. If the damping of the excited eigenmodes is sufficiently small, the result can be large, slow oscillations or problematic high-frequency vibrations.

The hydrodynamic modules of most floating wind CAE tools neglect radiation and diffraction forces beyond first order. This paper proposes an analysis methodology to quantify the second-order effects on offshore floating turbines, based on the methodology used in the offshore oil and gas industry. However, there are a number of reasons why wind turbines are different from oil and gas installations. First, the dynamics of a wind turbine are significantly influenced by aerodynamic forces (treated in a very simple way for other offshore structures) and the properties of the control system. Second, the wind turbine does not behave like a rigid-body structure. Last but not the least, in comparison to oil and gas platforms, floating wind turbines are smaller volume structures, for which viscous effects may be more important. The questions to be answered in this paper are therefore the following: Should second-order effects be included in floating wind simulation tools in the future, or do the assumptions that justify the disregard of higher-order effects for most traditional offshore structures also hold for wind turbines? How appropriate is the methodology commonly used in the offshore industry for analysis of offshore wind turbines?

There are very few previous studies applying second-order hydrodynamic theory to floating wind turbines. A report from the UpWind project [11] provides a summary of the theory of second-order hydrodynamics, and some results for the first- and second-order hydrodynamic coefficients for the OC3-Hywind spar buoy and a semisubmersible. Agarwal [1] investigated second-order effects on a monopile structure in shallow water, and used second-order wave kinematics in combination with Morison's equation to compare linear and nonlinear effects. This approach is however limited to bottom-mounted

slender cylinders. In the DeepCwind model tests performed at the MARIN wave basin in Wageningen, Holland, second-order effects were thought to have been observed, as reported in [3] and [4]. The significance of these effects inspired new interest in the loads and responses of floating wind turbines that are induced by second-order hydrodynamics.

This paper introduces a general methodology for the assessment of second-order effects on floating turbines, accounting for system geometry, as well as linearized system properties described by the system mass, damping and stiffness matrices. The proposed methodology is used to simulate the influence of second-order effects on two different floating wind turbine concepts, a spar and a TLP, both supporting the NREL 5-MW baseline wind turbine. Results for these systems are presented and analyzed in order to answer the questions posed above.

The remainder of this paper is organized as follows: Section 2 details the assessment methodology. Section 3 describes the properties of the two studied wind turbine concepts, and the results of the assessment are presented in Section 4. Conclusion and an outlook to future work are found in Section 5.

2. Modeling approach

In this paper, two simulation tools used for the simulation of floating wind turbines, FAST and WAMIT, have been used. FAST is a wind turbine CAE tool developed by NREL. The tool is open source and publicly available [13]. FAST predicts the coupled dynamic response of an entire wind turbine system nonlinearly in the time domain, taking aerodynamics, structural elasticity, control system and hydrodynamics into account.

WAMIT is a commercial 3D panel code designed to compute hydrodynamic loading from the radiation and diffraction problem in the frequency domain [16]. It is widely used in the offshore industry, and is capable of solving both the first- and second-order hydrodynamic problem for a rigid structure of arbitrary geometry.

Below, an outline of the current approach for simulation of hydrodynamic forces on floating offshore wind turbine using these two tools is given. Further, the extension to the current analysis methodology needed to assess second-order forces and motion response is presented.

2.1. Current simulation approach including first-order hydrodynamics

Currently, the coupled response of floating offshore wind turbines is simulated in FAST with first-order hydrodynamic quantities determined in WAMIT or a similar program. The first step in such an approach is to calculate the hydrostatic restoring, the frequency-dependent hydrodynamic added mass and damping matrices from wave radiation, as well as the frequency- and direction-dependent hydrodynamic force coefficients from wave diffraction. This is done in WAMIT, based on the geometry of the submerged portion of the floating platform. In a second step, the hydrodynamic quantities are given as an input to the time-domain simulation in FAST, together with models of the wind turbine (including structural, aerodynamic and control system properties), the floating platform and the mooring system. For a specific simulation, FAST also needs input describing the environmental conditions, more specifically the wind speed and the sea state.

The main benefit of this approach is that FAST solves the equations of motions in the time domain. This is the key characteristic that allows the transient behavior and the nonlinear coupled dynamics of the platform, tower and rotor to be accounted for in the simulation.

2.2. Simulation approach to include second-order hydrodynamics

One important property of the first-order hydrodynamic forces is that they only depend on the geometry of the structure and not on the motion response to the incoming waves. It is thus possible to

compute the first-order hydrodynamic quantities in WAMIT without solving any equations of motion. However, the forces arising from the second-order problem depend not only on the structure's geometry, but also on the solution to the first-order equations of motion. Therefore, the first-order motion response must be given in the frequency domain before second-order forces can be computed. The solution is typically given in the form of response-amplitude operators (RAOs), which describe the motion response as a function of wave amplitude and wave frequency. The computation of the RAOs is an integral part of a second-order calculation in WAMIT, where the first-order equations of motions are solved in the frequency domain. Because FAST at the moment is not configured to make use of second-order force inputs, the second-order equations of motion are also solved by WAMIT in the frequency domain and output as second-order RAOs. The RAOs can be converted into a time-domain response by assuming a specific sea-state with a given wave spectrum. Wind speeds are not needed by WAMIT, as aerodynamics cannot be accounted for. The complete approach is outlined in Figure 1.

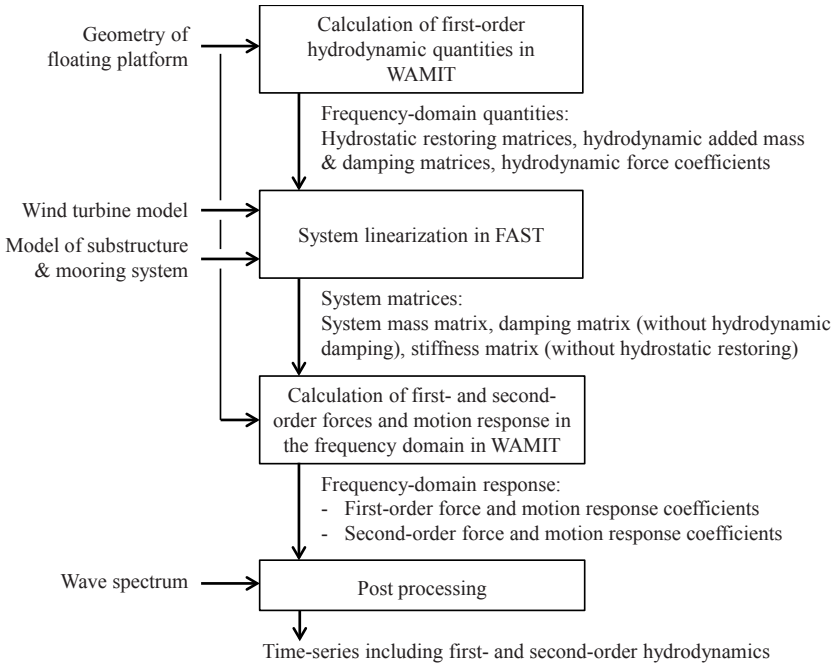

Figure 1 Procedure to analyze second-order effects with WAMIT and FAST.

To be able to solve the equations of motion, the system mass, damping and stiffness matrices of the wind turbine must be imported to WAMIT. These matrices are computed by the linearization procedure in FAST, which needs the same hydrodynamic inputs as for the time-domain simulation described in the former section to calculate the system matrices and system eigenfrequencies correctly. The linearized system properties output from FAST include contributions from the turbine (mass/inertia, aerodynamic damping/stiffness, gyroscopics), the substructure (mass/inertia) and the mooring system (stiffness properties). Any hydrodynamic contribution in the system matrices are removed before they are input to WAMIT to avoid counting these contributions twice.

The solution of the equations of motion in the frequency domain imposes some important limitations on the methodology. In the frequency domain, only steady-state, oscillatory forces can be taken into account and any non-linear effects are ignored. This eliminates the possibility to compute transient

behavior and to properly account for the influence of aerodynamics, control system actions, viscous drag, or other non-linear characteristics of the system (e.g. platform set-down for TLPs). Another important limitation to the calculation in WAMIT is that the structure is modeled as a rigid-body. The substructure could have been modeled as a flexible body using generalized modes, but this feature of WAMIT does not apply to any part of the structure outside of the water. The turbine flexibility, which is of higher importance to the response of the structure, can therefore not be included in WAMIT.

3. Properties of the analyzed wind turbine concepts

3.1. OC3-Hywind Spar

The first of the two analyzed floating wind turbine concepts is the OC3-Hywind spar. The spar buoy is a long, slender cylinder, which relies on a low center of gravity for stability. The considered configuration is a modified version of the full-scale 2.3-MW floating wind turbine that is built and operated by Statoil close to the southwest Norwegian coast. The platform model is the same that was used in the OC3 project and is described in [6]. The OC3-Hywind platform is designed to carry the NREL 5-MW reference wind turbine, which was developed to provide specifications for a model representative of a utility-scale multi-megawatt wind turbine [8]. The tower of the reference turbine was slightly changed to fit on the floating platform, and the control system was adapted to accommodate the floating platform motion. The properties of the new tower and controller, as well as other properties specific to the floating system are described in [6].

3.1.1. WAMIT model

The geometry of the OC3-Hywind substructure was modeled with quadrilateral panels. Because the spar has two planes of symmetry, only one quarter of the structure needs to be modeled, leading to shorter simulation time within WAMIT. A cosine-spaced mesh was used, giving a panel distribution with smaller panel size close to sharp edges or close to the free surface. This yields more accurate results for the same number of panels compared to equally sized panels [10]. The number of panels used to model the turbine and the free surface was chosen based on results from simulation convergence tests, which were performed in a way similar to that described in [14]. Using the finest discretization as a benchmark, all first-order and difference-frequency results seem to have an error of at most 2%. For the sum-frequency results, the largest error is in the order of 6%. More information regarding the convergence tests and the results can be found in [15].

3.1.2. Derivation of system matrices and system eigenfrequencies in FAST

The FAST model of the OC3-Hywind is provided by NREL. This model was used for all simulations of the OC3-Hywind in FAST. The mass, damping and stiffness matrices were derived through the FAST linearization process, with input from first-order hydrodynamic simulations in WAMIT. The linearized system parameters come from a case without any aerodynamic excitation.

The system eigenfrequencies are derived using the method outlined in [7]. WAMIT is not able to model turbine flexibility, Therefore any effects due to tower or blade flexibility will not be included when the equations of motion are solved. To see how the eigenfrequencies change depending on whether the tower and blades are modelled as flexible or rigid, the eigenfrequencies are computed for both cases. For the OC3-Hywind, the difference is insignificant. The eigenfrequencies for the case with a rigid tower and blades is seen in Table 1 (left). It should be noted that the OC3-Hywind spar is designed to have eigenfrequencies below the frequency range of the incident waves, i.e. below 0.25 rad/s. The exception is the platform-yaw degree of freedom, which is not significantly influenced by wave excitation but rather

by turbine effects like rotor gyroscopics. Due to the low eigenfrequencies, it can be expected that difference-frequency excitation from the waves might have an effect on the spar, while the effect of sum-frequency excitation will be negligible.

3.2. UMaine TLP

The second floating wind turbine concept analyzed here is a TLP developed by the University of Maine for use in the DeepCwind project. The TLP is a rather shallow structure, which relies on the mooring system, the so-called tension legs, to remain stable. The turbine carried by the TLP platform is the same NREL 5-MW reference turbine that was used for the OC3-Hywind, with slightly different tower and control system properties as described in [8]. Further information about the TLP system can be found in [3] and [4].

3.2.1. WAMIT model

Due to the rather complicated shape, the geometry of the TLP was modeled using MultiSurf, a CAD program. As with the OC3-Hywind, cosine spacing was used to get a better trade-off between computational effort and accuracy, and the number of panels was chosen based on convergence tests [14]. Again using the finest discretization as a benchmark, all first-order results seem to have converged to an error of less than 5%. For the sum- and difference frequency results, the error is harder to quantify, as computational effort put a rather strict limit on the highest number of body panels that could be tested. Experience from the spar computations do, however, indicate that the error should be in the order of less than 10%. More information regarding the convergence tests and the results can be found in [15].

3.2.2. Derivation of system matrices and system eigenfrequencies

The FAST model used to simulate the TLP is the model that was used to develop the model-scale TLP wind turbine for the DeepCwind project. The system matrices and system eigenfrequencies were derived in the same way as for the OC3-Hywind, using FAST for linearization and the same assumptions. Also for the TLP, the system eigenfrequencies were derived for both rigid and flexible turbine tower and blades. The difference between the two cases is more significant than for the OC3-Hywind, as can be seen from the results presented in Table 1 (right).

Table 1: Eigenvalues of OC3-Hywind Spar (left) and for UMaine TLP (right) with rigid and flexible wind turbine blades and tower.

Degree of freedom	OC3-Hywind		UMaine TLP		
	Eigenfrequency [rad/s]		Eigenfrequency (rigid) [rad/s]	Eigenfrequency (flexible) [rad/s]	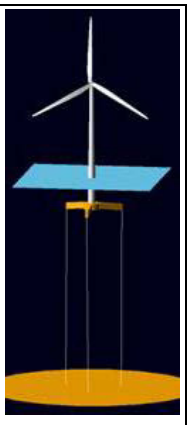
Surge	0.051		0.156	0.156	
Sway	0.051		0.156	0.156	
Heave	0.204		5.975	5.948	
Roll	0.215		3.388	2.005	
Pitch	0.215		3.392	2.021	
Yaw	0.761		0.374	0.374	

Whereas the eigenfrequencies in surge, sway, heave and yaw remain almost the same, a significant shift of the pitch and roll frequencies from about 3.4 rad/s with a rigid tower to about 2.0 rad/s with a

flexible tower is observed. This shift is due to a coupling between tower-bending and platform-pitch, an effect which has already been described for the NREL/MIT TLP in [12]. Because there is no possibility to model the flexible turbine tower within WAMIT, the results for the pitch and roll degrees of freedom may be inaccurate. It should also be noted that the eigenfrequencies of the UMaine TLP in heave, roll and pitch are above the incident wave frequency range. For these degrees of freedom, sum-frequency excitation can be expected to be of importance.

4. Results

In this section, the magnitudes of the first- and second-order forces and response are compared for both concepts. Excitation from second-order hydrodynamics and aerodynamics is compared for the OC3-Hywind spar.

The first-order quantities were computed for incident wave frequencies in the range 0.005 to 5 rad/s. Due to the high computational effort needed to compute the second-order solution, the second-order quantities were computed for combinations of 21 different frequencies in the range from 0.26 to 1.5 rad/s.

4.1. Comparison of first- and second-order response in a specific sea state

The frequency-domain coefficients that are output from WAMIT are normalized such that they provide the force and motion response per wave amplitude. The first-order quantities are normalized by one incident wave amplitude, whereas the second-order quantities are normalized by pairs of incident wave amplitudes. Therefore, a direct comparison of first- and second-order quantities is only possible after a sea state with quantified wave amplitudes has been chosen. To get the force or motion experienced by the platform in the ocean, the coefficients are multiplied by the complex amplitude of the incident waves. The complex wave amplitude $A_m = a_m e^{i\varphi_m}$ belonging to a wave with frequency ω_m is specified by a magnitude a_m and a random phase φ_m. The wave amplitude a_m at a given frequency ω is determined directly and uniquely from the wave spectrum $S(\omega)$. The wave phase φ_m is uniformly distributed between 0 and 2π and based on selection of a random wave seed.

There are many pairs of waves that contribute to the overall second-order force (and motion) at a given frequency because there exist many pairs of wave frequencies that share the same sum or difference frequency. The quantity of interest is, however, the total second-order force or motion response, which is given by the complex sum over all contributions at a given frequency. This summation is given by

$$\left|F_{total}{}^{\pm}(\omega_k{}^{\pm})\right| = \left|\sum_{\omega_m \pm \omega_n = \omega_k{}^{\pm}} f_{mn}{}^{\pm} A_m A_n\right| = \left|\sum_{\omega_m \pm \omega_n = \omega_k{}^{\pm}} \left|f_{mn}{}^{\pm}\right| a_m a_n e^{i(\varphi_{mn}{}^{\pm} + \varphi_m + \varphi_n)}\right| \quad (1)$$

Here $f_{mn}{}^{\pm} = \left|f_{mn}{}^{\pm}\right| e^{i\varphi_{mn}{}^{\pm}}$ is the complex second-order force coefficient of the wave pair with frequencies ω_m and ω_n. Because the incident wave phases φ_m and φ_n are random and depend on the chosen wave seed, the total force contribution differs between realizations. To get an impression of the range and variation of the total magnitudes, the summation is done for 15 different wave seeds. The result for the surge and heave degrees of freedom is shown in Figure 2 for the OC3-Hywind spar and in Figure 3 for the UMaine TLP. The wave spectrum in this study is a Pierson Moscowitz wave spectrum with H_s = 3.66 m and T_p = 9.7 s, which represents a moderate environmental condition with an operating turbine.

For the OC3-Hywind spar, the second-order forces are very small compared to the first-order forces. However, where the difference-frequency forces coincide with the eigenfrequencies of the structure, some motion response is seen. Second-order difference-frequency response in heave is most significant compared to the first-order response. This is because the second-order excitation at the heave

eigenfrequency is higher compared to the overall first-order excitation than for the surge or pitch directions. The difference-frequency response of the surge degree of freedom has two peaks. The lower one is response due to excitation at the surge eigenfrequency, and the upper one due to excitation of the pitch eigenfrequency, to which the surge response is coupled. Comparing the difference-frequency coefficients for the different wave pairs, the off-diagonal coefficients are found to be much larger than the coefficients along the diagonal. This is as expected, as the deep penetration of the second-order diffraction potential means that it has a relatively large effect on the forces on deep draft structures compared to the forces arising from quadratic interactions of first-order quantities.

The second-order forces are much higher in magnitude for the UMaine TLP than for the OC3-Hywind spar, and the motion response is therefore also much more significant. In heave, the sum-frequency forces are of the same or even higher magnitude as the first-order forces, meaning that the sum-frequency response actually dominates the overall heave motion response. Interestingly, this happens even without excitation of an eigenfrequency. For surge, the response due to difference-frequency excitation at the eigenfrequency dominates the overall response. Due to the coupling between pitch and surge, the same peak is seen in the plot for the pitch degree of freedom. One reason for this very large response might be that viscous drag is neglected. For such oscillations in surge, the viscous drag could be expected to be relatively high, especially since the TLP has relatively many slender parts. It should be noted that the pitch eigenfrequency (3.4 rad/s) is outside the range of sum-frequency excitation, and thus there is no sum-frequency response in pitch. If it would be possible to model the flexibility of the turbine tower in WAMIT, the pitch eigenfrequency would shift to 2 rad/s, and we could expect to have significant sum-frequency response at this frequency as well.

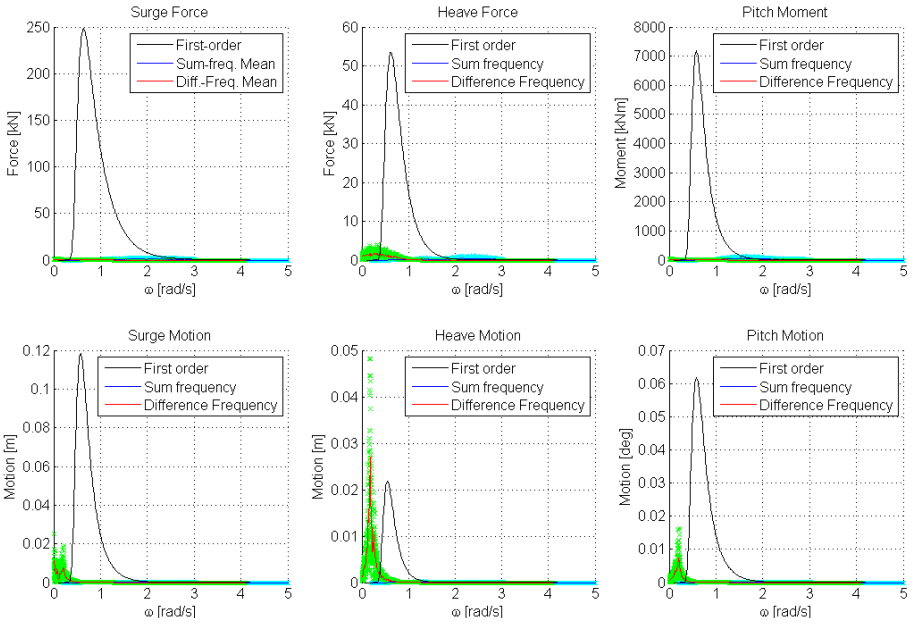

Figure 2 First- and second-order forces (upper part) and motion responses (lower part) for the OC3-Hywind spar.

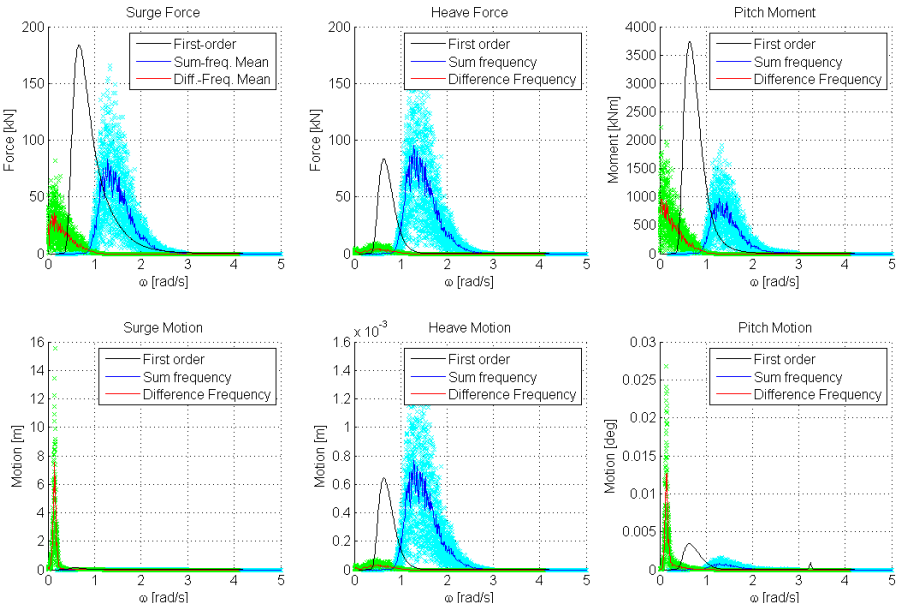

Figure 3 First- and second-order forces (upper part) and motion responses (lower part) for the UMaine TLP.

The first-order force and motion response is represented by a single black line because it does not depend on the random phase and therefore does not vary between realizations. The single points (cyan for sum-frequency results and green for difference-frequency results) represent the total force or motion response at a certain sum or difference frequency for one realization of the sea state. The blue line (sum frequency) and the red line (difference frequency) represent the mean over all realizations.

4.2. Comparison of the effects from second-order hydrodynamics and aerodynamics

A floating turbine experiences forces not only from hydrodynamics but also from aerodynamics. Aerodynamic loading on the rotor is known to produce slowly varying excitation in a frequency range similar to that of the difference-frequency hydrodynamic forces, and with a magnitude that is possibly substantially higher. To create a case for comparison between aerodynamic and difference-frequency hydrodynamic response, time series from FAST simulations (with aerodynamic and first-order hydrodynamic forces) and time-series based on WAMIT first- and second-order RAOs are compared. The FAST time-series were based on turbulent wind input data generated by TurbSim [5], and was run with rigid turbine tower and blades. The wave spectrum used for both the FAST time series and the time-series based on WAMIT RAOs was a Pierson-Moskowitz spectrum generated by FAST.

4.2.1. Comparison of mean-drift force and mean wind turbine thrust

The mean-drift force is a constant force that arises from interactions of oscillations with the same frequency. To compute the mean-drift force, all components with zero difference frequency are summed. This sum (given in Eq. (2)) can be done without taking the random phases into account (as was done in the summation in Eq. (1)) because the random phases of two identical components cancel out. F_{mm} is the mean-drift force coefficient for the incident wave frequency ω_m, with magnitude f_{mm} and phase φ_m.

$$F_{mean} = \sum_m A_m A_m{}^* F_{mm} = \sum_m a_m a_m e^{i(\varphi_m - \varphi_m)} f_{mm} e^{i(\omega_m - \omega_m)} = \sum_m a_m{}^2 f_{mm} \qquad (2)$$

The mean-drift force and the mean turbine thrust are compared for 12 different environmental conditions identified in [15]. The mean-drift force was calculated as described in Eq. (2), and the mean wind turbine thrust was calculated from the FAST time series for each of the given environmental conditions. The results are shown in Figure 4 for the OC3-Hywind spar. For the cases where the turbine is operating, the mean-drift force is less than 1% of the rotor thrust. In more severe environmental conditions, where the turbine is idling and the rotor thrust is significantly lower, the mean-drift force amounts to about 10-15 % of the rotor thrust. However, this is still low enough to neglect the mean-drift force in general. The significance of the mean drift force would likely be even smaller if the direct wind drag load on the tower, which has not been considered here, would be included in the simulation.

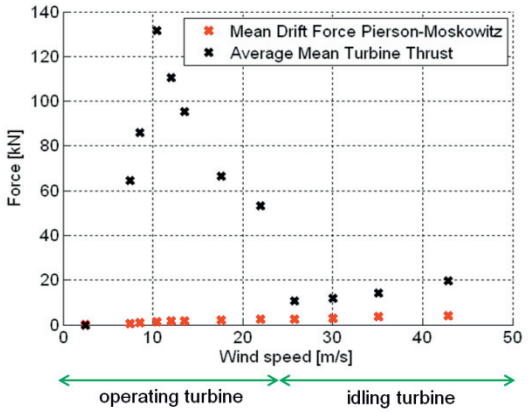

Figure 4 Comparison of mean-drift force and mean thrust force for the OC3-Hywind spar.

4.2.2. Comparison of motion response due to excitation from second-order and aerodynamic forces

In this section, the importance of the difference-frequency forces on the motion response is compared to the importance of aerodynamics. The power-spectral densities (PSDs) of the motion response in surge, heave and pitch were computed for the same 12 environmental conditions as the mean-drift force. The results shown in Figure 5 are the PSD of the surge response of the OC3-Hywind. The sea state is the same as in Section 4.1, with H_s = 3.66 m, T_p = 9.7 s and mean wind speed at hub height equal to 17.6 m/s.

The time-series from FAST and the time-series based on the frequency-coefficients from WAMIT give the same response in the incident wave frequency band (0.25 – 1.5 rad/s) in all modes of motion and for all sea states, confirming that the first-order wave excitation is the same for both systems, and that the first-order hydrodynamic excitation is dominating the motion response in this frequency range.

The main difference between the time-series from FAST, which contains excitation from aerodynamic forces, and the time-series based on frequency-domain coefficients from WAMIT, which contains excitation from second-order hydrodynamic forces, is seen in the low-frequency domain. The response due to aerodynamic excitation is several orders of magnitude higher than the response due to second-order hydrodynamic effects, and dominates the overall response of the turbine. This holds for all considered conditions and not only for the surge degree of freedom, but also for heave and pitch.

From these results, it is concluded that in the case of the OC3-Hywind spar, aerodynamic excitation has a much more significant effect on the motion response than the excitation from difference-frequency hydrodynamic forces.

In the high-frequency domain above 1.5 rad/s, the response due to both wind and wave excitation is orders of magnitude smaller than at lower frequencies. High-frequency excitation seems to be of little importance to the spar motion response, and the sum-frequency wave excitation is even less important

than high-frequency wind excitation. However, these results are based on a rigid turbine configuration, and could be different if structural dynamics were included. Also, no interactions between the second-order wave loading and high-frequency wind loading could be simulated in the current set-up.

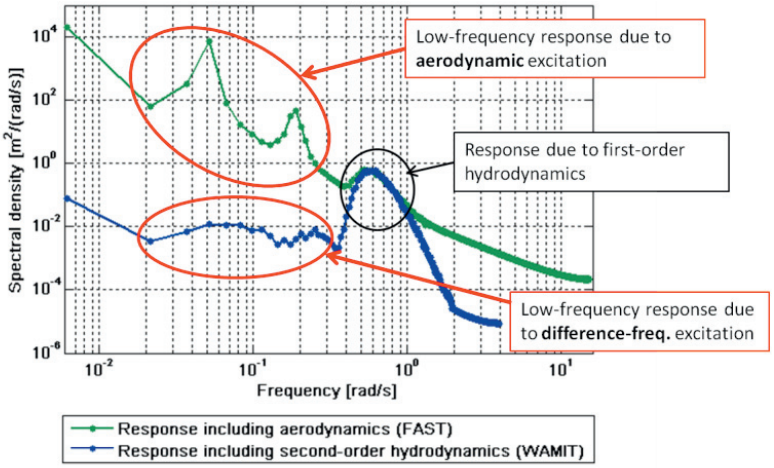

Figure 5 Surge response of the OC3-Hywind spar due to first-order hydrodynamic excitation combined with aerodynamic excitation (green) or second-order hydrodynamic excitation (blue). Sea state: Hs=3.66 m, Tp=9.7s, mean wind speed at hub height=17.6 m/s.

5. Conclusions

In this paper, a method to assess the effect of second-order hydrodynamics on floating offshore wind turbines has been presented. The proposed method relies mainly on simulation by the frequency-domain tool WAMIT, and is based on the simulation methodology typically applied to more traditional offshore structures, with the addition of inputs derived from the wind turbine CAE tool FAST.

Using the proposed method, the importance of the second-order effects has been assessed for the OC3-Hywind spar and the UMaine TLP. More results than was presented here can be found in [15]. The second-order forces are very small for the OC3-Hywind spar, but where the forces excite eigenfrequencies, some second-order motion response is seen. For the UMaine TLP, the second-order forces are quite high, leading to a higher motion response. In heave, the sum-frequency effects dominate the overall motion response, even without exciting any eigenfrequencies.

In a second step, the second-order effects have been compared to aerodynamic effects for the OC3-Hywind spar, to assess their relative importance in more realistic environmental conditions. The mean-drift force was found to be insignificantly small compared to mean turbine thrust. A comparison between the motion response induced by aerodynamics and second-order hydrodynamics also revealed that aerodynamics dominate the response of the turbine in the low-frequency domain, and that the motion response due to difference-frequency excitation is negligible in comparison. A similar comparison of the relative importance of second-order effects and aerodynamics for the TLP has not yet been performed, but is part of future work. As aerodynamics are introduce less energy to the system at high frequencies, the sum-frequency effects of the TLP are likely to be more important compared to other sources of excitation than the difference-frequency excitation.

In the process of simulating the second-order effects of the OC3-Hywind spar and UMaine TLP, some limitations to the proposed method have been identified: First, the tower flexibility cannot be taken into account in WAMIT, leading to inaccuracies in the simulation of second-order quantities for structures where the tower flexibility couples to and influences the eigenfrequencies in pitch and roll (i.e. TLPs).

One possible solution to this would be to derive RAOs based on FAST output, and import these to WAMIT. However, this solution would require changes to the WAMIT source code. Another possibility might be to tune the FAST inputs to WAMIT, i.e. the stiffness matrix, to get the first-order RAOs predicted by WAMIT to match those derived from FAST. The second drawback is that viscous effects, which would likely damp some of the second-order motion response, are not accounted for when solving the equations of motion in WAMIT. One solution would be to linearize the viscous drag contribution and include this in the system damping matrix which is input to WAMIT. This is currently being tested. A more thorough solution would be to import second-order force coefficients from WAMIT to FAST in a way similar to the first-order coefficients. This would require a change in FAST and is currently being worked on. It would allow simulation of the complete coupled response of the turbine, including first- and second-order hydrodynamics, as well as viscous drag and aerodynamics.

References

[1] Agarwal, P., Simulation Structural Reliability Offshore Wind Turbines, Ph.D. Dissertation, University of Texas at Austin, Austin, TX, August 2008

[2] de Ridder, E.J., Koop, A.H. and Doeveren, A.G., DeepCwind Floating Wind Turbine Model Tests, Report No. 24602-1-OB, MARIN, Wageningen, Netherlands, December 2011

[3] Goupee, A.J., Koo, B., Kimball, R.W. and Lambrakos, K.F., Experimental Comparison of Three Floating Wind Turbine Concepts, Proceedings of the 31st International Conference on Ocean, Offshore and Arctic Engineering, Rio de Janeiro, Brazil, June 10-15, 2012

[4] Goupee, A.J., Koo, B., Lambrakos, K.F. and Kimball, R.W., Offshore Wind Energy: Model Tests for Three Floating Wind Turbine Concepts, Proceedings of the Offshore Technology Conference held in Houston, Texas, USA, 30 April–3 May 2012.

[5] Jonkman, B., TurbSim User's Guide: Version 1.50, NREL/TP-500-46198, Golden, CO, National Renewable Energy Laboratory, September 2009

[6] Jonkman, J., Definition of the Floating System for Phase IV of OC3, NREL/TP-500-41958, Golden, CO: National Renewable Energy Laboratory, November 2007.

[7] Jonkman, J. M. and Buhl, M. L., Jr., FAST User's Guide, NREL/EL-500-38230, Golden, CO: National Renewable Energy Laboratory, August 2005.

[8] Jonkman, J., Butterfield, S., Musial, W., and Scott, G., Definition of a 5-MW Reference Wind Turbine for Offshore System Development, NREL/TP-500-38060, Golden, CO: National Renewable Energy Laboratory, February 2009

[9] IEA Wind Task 23, Offshore Wind Technology and Deployment, "Subtask 2: The Offshore Code Comparison Collaboration, Final Report", http://www.ieawind.org/task_23/23_FinalReports/Subtask2_Final_Report.pdf

[10] Lee, C.-H., Newman J.N., Kim, M.H., and Yue, D.K., The computation of second-order wave loads, OMAE Conf., Stavanger, Norway, 1991

[11] Lucas, J., UpWind Project: Comparison of a First- and Second-Order Hydrodynamic Results for Floating Offshore Wind Structures, Garrad Hassan & Partners Ltd, Bristol, UK, January 2011

[12] Matha, D., Model Development and Loads Analysis of an Offshore Wind Turbine on a Tension Leg Platform, with a Comparison to Other Floating Turbine Concepts, NREL/SR-500-45891, Golden, CO: National Renewable Energy Laboratory, February 2010

[13] National Wind Technology Center, URL: http://www.nrel.gov/wind/, Simulation code download URL: http://wind.nrel.gov/designcodes/simulators/

[14] Newman, J.N., Sensitivity of wave loads to the discretization of bodies, BOSS (Behaviour of Offshore Structures), ss. 50-64, London, 1992

[15] Roald, L.A., The Effect of Second-Order Hydrodynamics on a Floating Offshore Wind Turbine, Master Thesis, ETH Zürich, 2012

[16] Wamit, Inc. (2002). WAMIT User Manual, Version 6.4., WAMIT Inc.